Interference Suppression Approaches Utilizing Phase-Only Control and Metaheuristic Algorithms: A Comparative Study

Le Thi Trang[1,2], Nguyen Van Cuong[1], and Tong Van Luyen[1(✉)]

[1] Hanoi University of Industry, Hanoi, Vietnam
luyentv@haui.edu.vn
[2] Electric Power University, Hanoi, Vietnam

Abstract. This paper evaluates interference suppression solutions using beamforming (BF) techniques based on phase control of the excitation signal for each element in the antenna array and metaheuristic algorithms. The metaheuristic algorithms investigated in this study include BA Algorithm (BA), Hybrid Particle Swarm Optimization-Gray Wolf Optimization (HPSOGWO), Multi-Verse Optimizer (MVO), and Jaya. Nulls are placed in the interfering directions on the radiation pattern of the equally spaced linear half-wavelength antenna array (Half-wave Dipole Uniformly spaced Linear Array-HDULA). The evaluation results have demonstrated that the interference suppression solutions based on metaheuristic algorithms are capable of suppressing sidelobes, maintaining the main lobe, and accurately imposing nulls in any interference direction. Furthermore, this evaluation has also shown that the solutions utilizing BA, HPSOGWO, and MVO outperform the Jaya-based ones in terms of computation time and null depth levels.

Keywords: Metaheuristic algorithms · Beamforming · Interference suppression · Null-steering · Half-wave dipole uniformly spaced linear array

1 Introduction

Today, the evolution of the fifth-generation (5G) mobile network has reached new heights, boasting expanded coverage, increased information traffic, reduced latency, and connection density with enormous bandwidth. This remarkable progress is proving to be a crucial driving force behind the development of the Internet of Things, ushering in an era where billions of sensors can seamlessly connect over the Internet [1–3]. However, amidst these advancements, a significant challenge that looms large for 5G networks is interference. The promise of 5G lies in its potential to deliver incredibly faster internet speeds compared to its predecessor, 4G. This leap is achieved through the utilization of wider bands and higher frequencies. Unfortunately, this progress also brings with it the vulnerability of high-frequency bands to interference and signal weakness when confronted with obstacles like buildings or trees. The deployment of 5G signals introduces

N. Thi Dieu Linh et al. (Eds.): ADHOCNETS 2023, LNICST 558, pp. 65–85, 2024.
https://doi.org/10.1007/978-3-031-55993-8_6

particular obstacles that need to be overcome to fully exploit the potential of this state-of-the-art technology. One notable issue is the vulnerability of 5G waves, which operate in the millimeter wave (mmWave) range, to being weakened or absorbed by physical structures. This characteristic can lead to signal loss or a reduction in strength as the waves pass through buildings and other obstacles. Interference from various electronic devices is another concern in 5G networks. With the expectation of supporting a multitude of devices concurrently, there is a risk of bandwidth contention and interference from other electronic gadgets within the environment. Additionally, when numerous base stations and connected devices are in close proximity, signals may interfere with each other, resulting in compromised performance and reduced connection speeds. To overcome these problems and challenges, it is crucial to focus on research and development efforts to create new technologies that enhance the network's ability to suppress interference. Improving performance and connection speed during the deployment and operation of 5G networks is paramount importance.

The effectiveness of 5G in the Internet of Things hinges on three pivotal elements: ensuring secure communication, enhancing overall performance, and achieving smooth transmission of substantial data volumes devoid of disruptions [4, 5]. To accomplish this, fast-response interference suppression solutions are essential for 5G wireless communication technology [6]. In the realm of information network processing, an integrated interference suppression solution holds paramount importance.

Several popular interference suppression solutions are available today, offering various advantages and capabilities. These solutions encompass various technologies such as digital encryption, error correction codes, information filtering, channel code usage, improved Multiple Input Multiple Output (MIMO) technology, the Maximum Ratio Combining (MRC) method, digital signal processing techniques, multi-user MIMO (MU-MIMO), and BF techniques. The beauty of these solutions lies in their versatility, as they can be combined and tailored according to the specific requirements and conditions of the information network, ensuring the highest performance and reliability [4, 7–9]. This paper places special emphasis on evaluating the interference suppression solution using BF. In the context of 5G mobile communication systems, BF assumes a vital role, boasting numerous advantages such as extended coverage, improved signal transmission quality, enhanced spectrum usage, and effective interference suppression capabilities.

The BF technique involves controlling the signal of each antenna element based on a predefined principle. The primary purpose of this control operation is to shape and direct the beam of the antenna array, achieving specific objectives such as generating and steering the main beam in a designated direction, modifying the sidelobe level, and establishing a "Null" region. The configuration and control of the antenna array's beams are effectively tailored to suit the communication system's requirements [10, 11]. In general, the received signal from each element can be adjusted in terms of magnitude, phase, or both magnitude and phase. Different control techniques, each with unique benefits and drawbacks, have been extensively utilized in practical applications. This paper focuses on a method that sets the "Null" region through phase adjustment and optimizes it using a metaheuristic algorithm to address specific limitations. This approach presents enhanced complexity and attractiveness for phase arrays since it leverages

existing controls without incurring additional costs. Furthermore, correcting the main beam's direction can be easily accomplished through phase weight adjustments [12, 13].

Metaheuristic techniques like BA, HPSOGWO, MVO, and Jaya have been utilized to address continuous optimization challenges. These algorithms are non-derivative methods and are known for their simplicity, adaptability, and capability to avoid getting trapped in local optima. They operate in a stochastic manner, beginning the optimization process by generating random solutions. Unlike Gradient search techniques, metaheuristics do not require the calculation of derivatives for the search space. They are both flexible and easy to comprehend due to their straightforward concepts and ease of implementation. These algorithms can be easily customized to suit specific problems. Moreover, owing to their inherent randomness, these techniques function like a black box, steering clear of local optima and efficiently exploring the search space. They achieve a balance between two critical processes: exploration and exploitation. During the exploration phase, the algorithms extensively explore potential search spaces, and subsequently, they conduct a local search in the identified promising areas [14].

BA is an optimization algorithm that draws inspiration from the foraging behavior of BAs in their natural environment. It mimics their use of echolocation techniques to detect prey, avoid obstacles, and determine locations in the darkness. During the search process, BAs interact and learn from each other by modifying their positions and velocities. By utilizing this process, BA becomes capable of finding optimal solutions for optimization problems. Introduced by Xin-She Yang in 2010, the algorithm has proven successful in solving a wide range of engineering problems [14–16]. HPSOGWO combines the exploration capability of Grey Wolf Optimizer (GWO) and the exploitation ability of Particle Swarm Optimization (PSO) to achieve enhanced performance in discovering optimal solutions [17]. It utilizes a population of agents to create a search space. The search process involves interactions among the agents, where PSO is employed to adjust their velocities and GWO is used to update their positions. MVO is a unique nature-inspired algorithm that draws inspiration from three cosmological concepts: white holes, black holes, and wormholes. It constructs mathematical frameworks based on these ideas to execute exploration, exploitation, and localized investigation within optimization challenges. The study outcomes have demonstrated the encouraging capacity of MVO to adeptly address practical issues encompassing unfamiliar search domains [18]. Jaya, on the other hand, is a relatively recent metaheuristic algorithm with a straightforward structure, needing only the population size and termination conditions for optimization. Due to these two characteristics, Jaya has found extensive applications in solving various optimization problems. However, when dealing with complex optimization problems, Jaya may become susceptible to getting stuck in local minima because of its single learning strategy and limited population information [19].

After the introduction, we will move on to the problem formulation. In this section, we will detail the specific issue that this research is focusing on. There will be a detailed description of how interference reduction will be performed using metaheuristic algorithms as well as phase control of the excitation signal for each element in the antenna array. Important aspects of the problem will be analyzed and outlined, ensuring that the reader has a clear view of the scope and goals of the research.

2 Problem Formulation

This paper will consider HDULA with a three-dimensional radiation pattern, depicted in Fig. 1, and an equidistant linear array of M uniformly spaced elements positioned along the axis y as illustrated in Fig. 2. Throughout the paper, the azimuth angle ϕ will be considered at 90°.

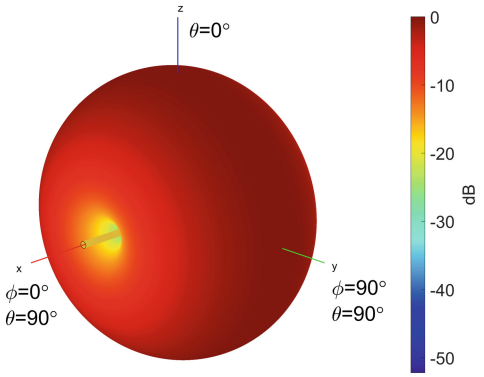

Fig. 1. 3D radiation pattern of a dipole antenna with a length equal to half of a wavelength.

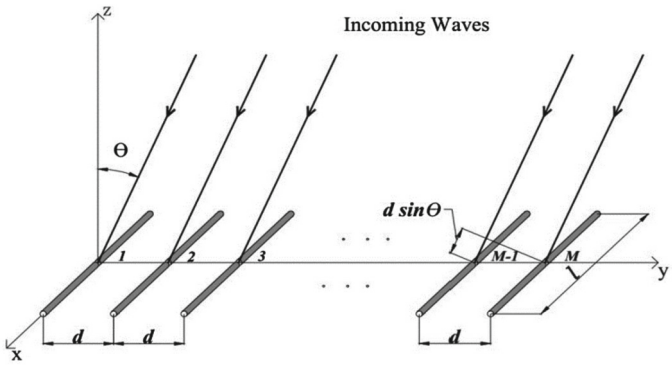

Fig. 2. The dipole antenna array comprises M elements.

The array factor of the HDULA can be represented as shown in references [20] and [21]:

$$AF(\theta) = \sum_{m=1}^{M} w_m e^{j(m-1)dk\sin(\theta)} \tag{1}$$

where:

- $w_m = a_m e^{j\delta_m}$: the complex current (or complex weight) excited at the m array element.

- a_m : the amplitude of the current at the m array element.
- δ_m: the phase of the current at the m array element.
- M: the total number of array element antennas in the array.
- $k = \frac{2\pi}{\lambda}$: the wave numbers.
- λ: the wavelength.
- $d = \frac{\lambda}{2}$: the distance between adjacent elements.

The expression for the array factor in Eq. (1) is as follows:

$$AF(\theta) = \sum_{m=1}^{M} a_m e^{j((m-1)dk\sin(\theta)+\delta_m)} \tag{2}$$

where $EF(\theta)$ is the array element pattern and $l = \frac{\lambda}{2}$ is the length of dipole.

This paper will use the technique of setting null as the phase control of the weights to obtain the optimal radiation pattern for interference suppression. The block diagram of interference suppression solutions based on beamformer is illustrated in Fig. 3, where the total number of elements in the array M is an even integer (M = 2N). Through the center of the antenna array, the amplitudes of the weights are chosen as an even symmetric function ($a_{-n} = a_n$), and the phase of the weights is chosen as an odd symmetric function ($\delta_{-n} = -\delta_n$) [22, 23]. As a result, through the main beam direction ($\theta = 0$), an antisymmetrical pattern is formed. So, when $a_{-n} = a_n$ and $\delta_{-n} = -\delta_n$, the array coefficient in (2) can be rewritten as:

$$AF(\theta) = 2\sum_{n=1}^{N} a_n \cos(knd\sin(\theta) + \delta_n) \tag{3}$$

The radiation pattern of the array $P(\theta)$ is calculated by the principle of multiplication, which is the product of the radiation pattern of the element $EF(\theta)$ and the array coefficient $AF(\theta)$[20]:

$$P(\theta) = EF(\theta)AF(\theta) \tag{4}$$

An optimization problem has the following form:

$$\begin{aligned} \text{minimize} \quad & f(\mathbf{x}), \quad \mathbf{x} = (x_1, \ldots, x_d)^T \in \mathbb{R}^d \\ \text{subject to} \quad & g_i(\mathbf{x}) = 0, \quad i = 1, \ldots, K \\ & h_j(\mathbf{x}) \leq 0, \quad j = 1, \ldots, N \end{aligned} \tag{5}$$

where $\mathbf{x}$ is the optimal variable vector to be found for the problem, the function $f(\mathbf{x})$ is the objective function, and the functions $g_i(\mathbf{x})$ with $i = 1, \ldots, K$ and $h_j(\mathbf{x})$ with $j = 1, \ldots, N$ are bound functions. A vector $\mathbf{x}*$ is said to be optimal or a solution to the problem if it has the smallest objective function value among the vectors satisfying the conditions of the constraint functions. That is, for any vector $\mathbf{z}$ where $g_1(\mathbf{z}) = 0, \ldots, g_k(\mathbf{z}) = 0$ and $h_1(\mathbf{z}) \leq 0, \ldots, h_n(\mathbf{z}) \leq 0$, then $f(\mathbf{z}) \geq f(\mathbf{x}*)$[15, 23].

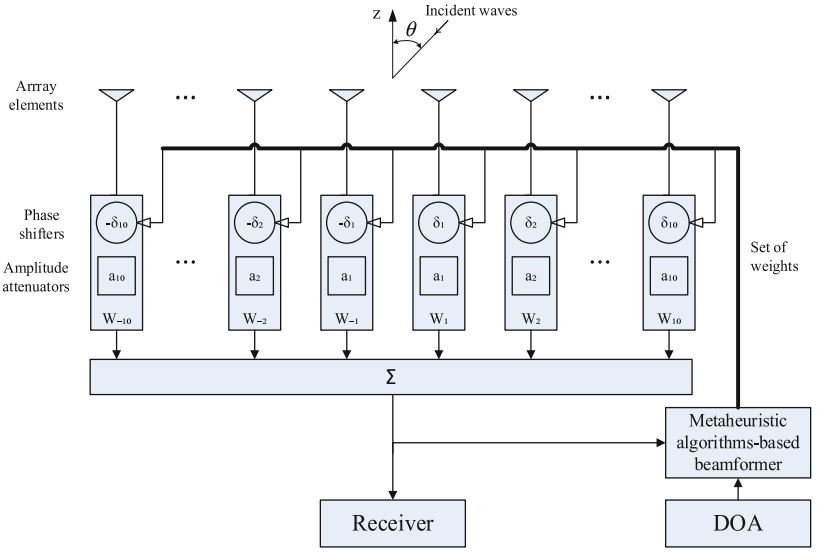

Fig. 3. Block diagram of beamformer based interferences suppression solutions with M = 2N

One of the ways to solve this optimization problem is to apply the Penalty Method [24]. Then, the constrained optimization problem (5) is transformed into the unconstrained optimization problem [15]:

$$\text{minimize}\, f(\mathbf{x}) + P_e(\mathbf{x}) \tag{6}$$

where $P_e(\mathbf{x})$ is the penalty component, defined as follows:

$$P_e(\mathbf{x}) = \sum_{i=1}^{K} \xi_i |g_i(\mathbf{x})| + \sum_{j=1}^{N} \upsilon_j \max\left(0, h_j(\mathbf{x})\right)^2 \tag{7}$$

The penalty parameters, or penalty coefficients, in this instance are $\xi_i > 0$ and $\upsilon_j > 0$. By transforming the constrained optimization problem into an unconstrained optimization problem, the penalty function method has the advantage of removing constraints. The new objective function specifically includes all binding functions. But as a result, there are more free parameters (penalty parameters) than values that must be identified in order to address the issue [15]. To simplify the implementation, assume that $\xi = \xi_i$ for every i and $\upsilon = \upsilon_j$ for every j. The new objective function can be rewritten as follows:

$$F(\mathbf{x}, \xi, \upsilon) = f(\mathbf{x}) + \xi \sum_{i=1}^{K} |g_i(\mathbf{x})| + \upsilon \sum_{j=1}^{N} \max\left(0, h_j(\mathbf{x})\right)^2 \tag{8}$$

It is evident that, when the equality constraint $g_i(\mathbf{x})$ is satisfied, their influence or contribution to the objective function is zero. However, when violated, they are penalized

by multiplying the penalty parameter ξ, and their contribution to the objective function increases significantly. Likewise, they are also true for the inequality constraints $h_j(\mathbf{x})$[15].

However, choosing the right values for penalty parameters can help solve the problem efficiently. Deciding which values are appropriate is a matter of concern. If the penalty parameters are too small, they can lead to insufficient penalties for violations; conversely, when the penalty parameters are too large, they can lead to excessive fines, from which the solution $\mathbf{x}$ too satisfies the condition the constraint functions instead of minimizing the objective function [15]. In this paper, the penalty parameter chosen is 10000.

According to the goal and requirements of the interference suppression solution, the beamformer is able to resist interference while maintaining the direction and width of the main beam and keeping the auxiliary beam at a pre-specified level. This means that the problem to be solved is a constrained optimization problem. Based on the above analysis, this problem can be expressed as an unconstrained optimization problem with a similar objective function (8) as follows:

$$F(\mathbf{x}, \xi) = f(\mathbf{x}) + \xi \sum_{i=1}^{K} |g_i(\mathbf{x})| \tag{9}$$

$$\Leftrightarrow F(\mathbf{w}, \xi) = f(\mathbf{w}) + P_e(\mathbf{w}) \tag{10}$$

where:

$$f(\mathbf{w}) = \sum_{\theta=-90^\circ, \theta\neq\theta_i}^{\theta=90^\circ} |P_o(\mathbf{w}, \theta) - P_d(\mathbf{w}, \theta)|^2 \tag{11}$$

$$P_e(\mathbf{w}) = \xi \sum_{i=1}^{N_i} |P_o(\mathbf{w}, \theta_i)|^2 \tag{12}$$

- The variable vector $\mathbf{x}$ is mapped by the weight vector $\mathbf{w}$;
- $f(\mathbf{w})$ is used to maintain the main beam's direction and width and keep the sub-beam at a pre-specified level;
- $P_e(\mathbf{w})$ is used to set nulls in the directions of the noisy signal on the radiation pattern;
- $P_o(\mathbf{w}, \theta)$ is the optimal radiation pattern obtained by optimization algorithms at θ.
- $P_d(\mathbf{w}, \theta)$ is the radiation pattern with the main beam and the desired SLL specified in advance at θ;
- $P_o(\mathbf{w}, \theta_i)$ is the optimal radiation pattern at θ;
- N_i is the total number of directions of the interfering signal;
- θ is the direction of the i$^{\text{th}}$ interferences signal with $i = 1, \ldots, N_i$

The final objective function of the issue can be restated as:

$$F(\mathbf{w}, \xi) = \sum_{\theta=-90^\circ, \theta\neq\theta_i}^{\theta=90^\circ} |P_o(\mathbf{w}, \theta) - P_d(\mathbf{w}, \theta)|^2 + \xi \sum_{i=1}^{N_i} |P_o(\mathbf{w}, \theta_i)|^2 \tag{13}$$

The existence of other antenna elements in the array has an impact on the radiation properties of the antenna elements during electromagnetic energy transmission in the array, including impedance and radiation pattern. Mutual coupling (MC: Mutual Influence) is the name given to this influence. In an adaptive array, taking into account the interaction effect is crucial since it has a direct impact on the array's effectiveness and performance, including the primary beam direction, SLL, and NDL. Therefore, the terms mutual impedance, coupling matrix, S parameter, or embedded element radiation (Embedded Element Pattern) have been used to describe the features of the interaction [20]. In order to analyze the interaction effect in HDULA in this paper, mutual impedance will be used.

For mutual impedance, if the source voltage $V = [V_1, V_2, ..., V_M]^T$ is taken, the input currents (excitation weight) $I = [I_1, I_2, ..., I_M]^T$ will be calculated using the following equation:

$$ZI = V \tag{14}$$

It can be determined using the induced electromotive force method, which is described in references, using Z as the mutual impedance matrix [20] and [21]:

$$Z = \begin{bmatrix} Z_{11} & Z_{12} & ... & Z_{1M} \\ Z_{21} & Z_{22} & ... & Z_{2M} \\ ... & ... & ... & ... \\ Z_{M1} & Z_{M2} & ... & Z_{MM} \end{bmatrix} \tag{15}$$

The mutual impedance (Z_{mn}) between element m and element n in the array is specified according to the information provided in references [20, 21, 24]:

$$Z_{mn} = \begin{cases} 73.129 + 42.546j & \text{if } m = n \\ 30[2C_i(u_0) - C_i(u_1) - C_i(u_2)] - 30j[2S_i(u_0) - S_i(u_1) - S_i(u_2)] & \text{if } m \neq n \end{cases} \tag{16}$$

where: $u_0 = 2\pi d$, $u_1 = 2\pi\sqrt{d^2 + 0.25} + \pi$; $u_2 = 2\pi\sqrt{d^2 + 0.25} - \pi$; the distance between the dipole elements is denoted as d, and C_i and S_i are given by:

$$\begin{aligned} C_i(u) &= \int_{\infty}^{u} \frac{\cos(x)}{x} dx \\ S_i(u) &= \int_{\infty}^{u} \frac{\sin(x)}{x} dx \end{aligned} \tag{17}$$

Based on Eqs. (7), (8), and (9), it is clear that the mutual impedance matrix $Z_{mn} \neq 0$ is non-diagonal, as $Z_{mn} \neq 0$ when $m \neq n$. Hence, the effective input currents I may not be identical to the voltages V. This leads to certain distortions in the array's pattern, affecting the nulls as well.

By applying noise suppression using an adaptive beamformer based on various nature-inspired algorithms. The adaptive beamformer requires global optimization algorithms to function properly. In this paper, algorithms BA, HPSOGWO, MVO, and Jaya will be applied to develop adaptive BF algorithms based on BA, HPSOGWO, MVO, and Jaya. To do so, the following steps will be performed:

- Map the location of the individual with the weight vector (including amplitude and phase), which are the variables to look for in the optimization process.
- Determine the search size of an instance: This value is equal to the product of the total number of weights and the number of binary bits representing a value.
- Limit the search value range of parameters.

Thus, the algorithm flowchart of an adaptive beamformer based on Jaya, HPSOGWO, BA, and MVO can be illustrated as Fig. 4, 5, 6 and 7, where the termination condition is the maximum number of iterations of the algorithm [25].

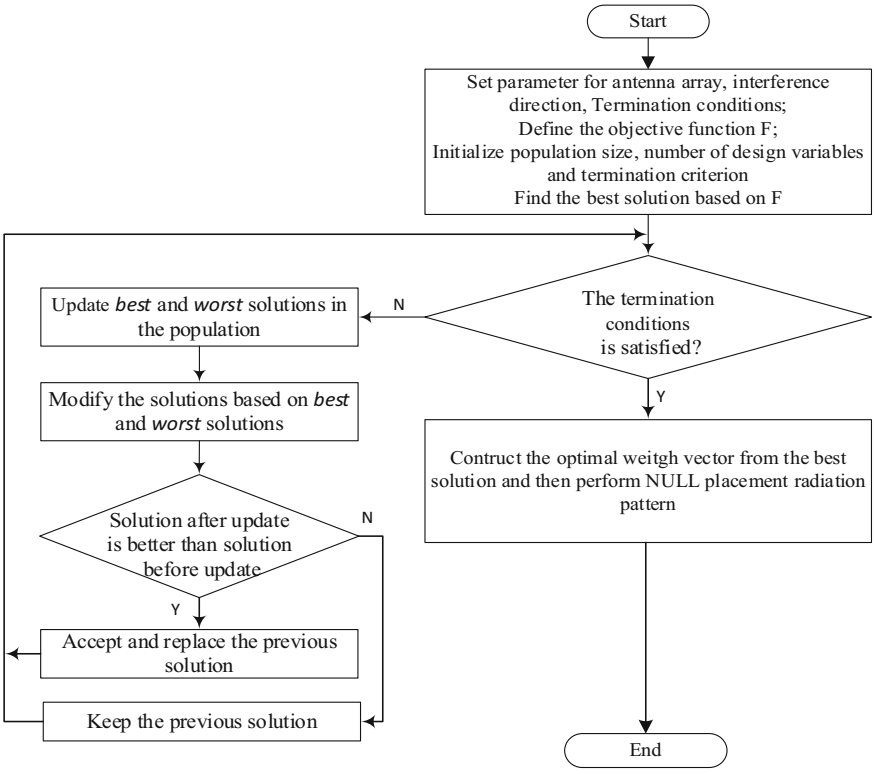

Fig. 4. Interferences suppression solutions based on Jaya

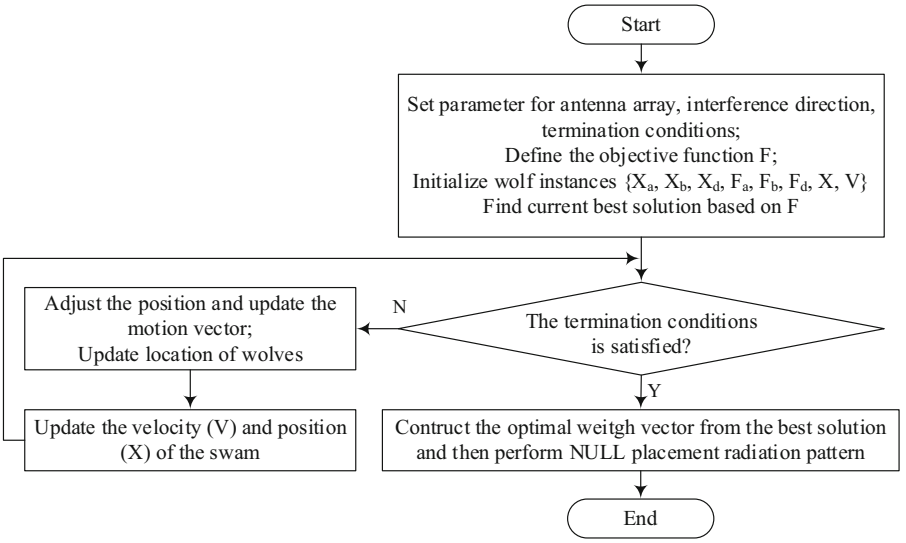

Fig. 5. Interferences suppression solutions based on HPSOGWO

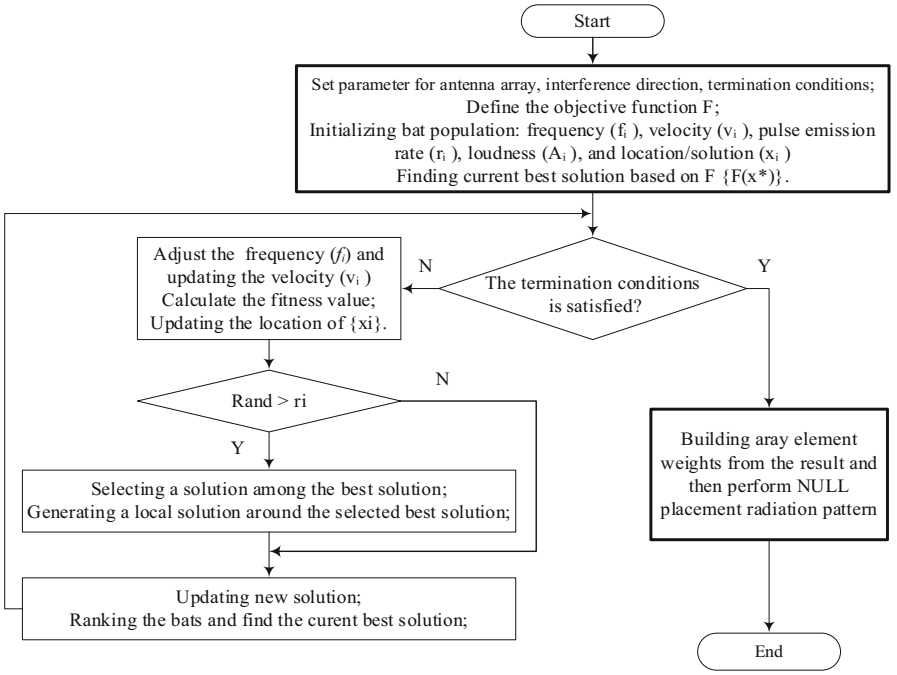

Fig. 6. Interferences suppression solutions based on BA

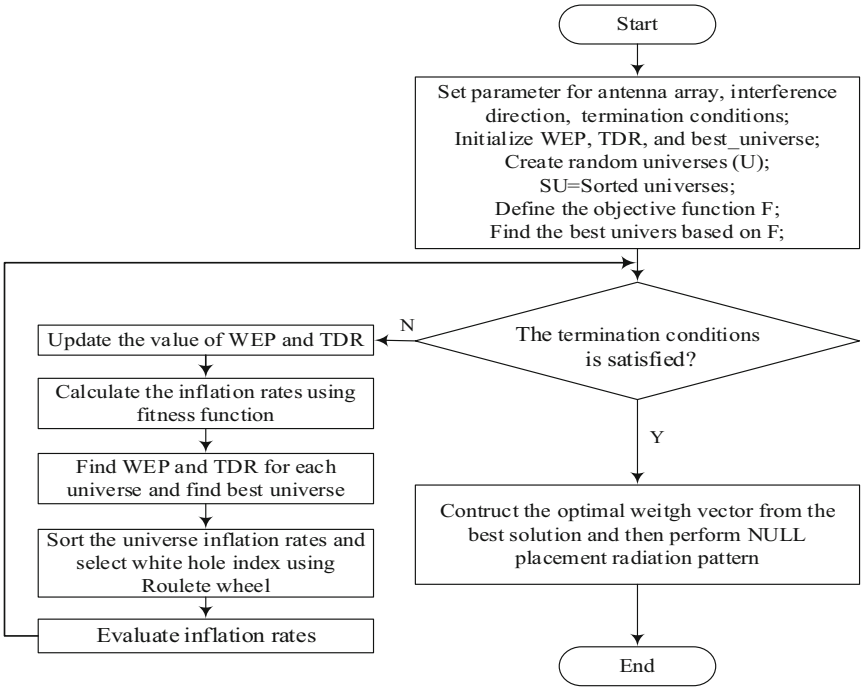

Fig. 7. Interferences suppression solutions based on MVO

After the problem is presented and analyzed, we perform eight simulation scenarios to evaluate interference suppression solutions using BF techniques based on phase control of the excitation signal for each element in the antenna array and metaheuristic algorithms. Eight simulation scenarios are presented, including convergence rate, placing single null, multiple nulls, and broad nulls on the radiation pattern in an ideal case, the impact of interference, steering the main beam, and the final scenario to evaluate the effectiveness of the solution as increasing the number of antenna elements will be done through the technique of setting null by phase adjustment based on BA, HPSOGWO, MVO, and Jaya algorithms.

3 Numerical Results

To evaluate interference suppression solutions using BF techniques based on phase control of the excitation signal for each element in the antenna array and metaheuristic algorithms, the study will investigate seven scenarios. The significant weight distribution in the Chebyshev array results in an optimized radiation pattern that effectively balances the sidelobe levels in the pattern and achieves a beamwidth for the first null point of the main beam in equally spaced arrays [26]. As a result, in this communication, the Chebyshev array factor has been selected as the desired pattern to regulate the *Sidelobe Level (SLL)* and beamwidth of the main beam. Initially, a Chebyshev array pattern exhibiting a SLL of 30 dB has been employed, consisting of 20 half-wave-dipole

elements with an inter-element spacing of $\lambda/2$. The step size of the theta angle in (1) is 1^o. The smaller θ is, the more accurate the main beam direction and the null point will be, but the time to find the optimal solution will increase.

In Fig. 8, it can be seen that the pop = 50, 100, 150, and 200 cases almost all reach the same objective function value at the loop of 50 and quickly reach $F \leq 2$. However, a large number of instances means increased computation time. Therefore, $pop = 100$ and $iter = 50$ will be selected for simulation for the remaining scenarios. The step size of a random walk is 0.01; boundary frequency values: $f_{min} = 0$ and $f_{max} = 1$.

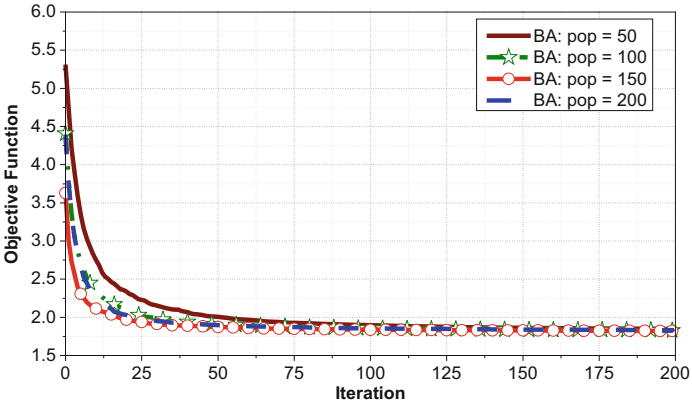

Fig. 8. Objective function of BA based solutions with different population sizes

Scenarios 1 and 2, named "Convergence Rate," were utilized to measure the convergence time of the objective function using the BA, HPSOGWO, MVO, and Jaya algorithms. Moving on, Scenarios 3 to 6 were used to assess the null steering capability of the waveform generator based on the BA, HPSOGWO, MVO, and Jaya algorithms in an ideal scenario disregarding mutual coupling effects. Expanding the evaluation, Scenario 6 was used to investigate the influence of mutual coupling, specifically employing the MVO algorithm. Scenario 7 focuses on main beam steering; the last scenario is used to evaluate the solution's effectiveness by increasing the number of antenna elements using the technique of setting null by phase adjustment based on the MVO algorithm. The simulation results for all scenarios are depicted in Figs. 8, 9, 10, 11, 12, 13, 14, 15, 16, 17, 18 and Tables 1 and 2.

A. *Convergence rate*

In Scenario 2, the convergence rate of the beamformer generator is evaluated using four algorithms: BA, HPSOGWO, MVO, and Jaya. Since the complexity of the algorithms is the same, the computation time and number of iterations to achieve a target objective function value are the parameters used to assess and compare these algorithms. The objective function values for each algorithm are illustrated in Fig. 9. The time taken for all four solutions to reach a target objective function value $(F <= 2.5)$ is 0.216 s for BA, 0.738 s for HPSOGWO, 1.364 s for MVO, and 3.659 s for Jaya, respectively. These evaluations were conducted on an Intel(R) Xeon(R) CPU @ 2.20GHz with

13 GB of RAM. The number of iterations for all four solutions to reach an equal objective function value *(F < = 2.5)* is 7, 12, 17, and 150 iterations, respectively, for BA, HPSOGWO, MVO, and Jaya algorithms. It is evident that BA converges faster compared to HPSOGWO, even faster than MVO, but significantly faster than Jaya. With such fast computation times, BA, HPSOGWO, and MVO can be considered promising solutions for real-time applications in wireless communication systems.

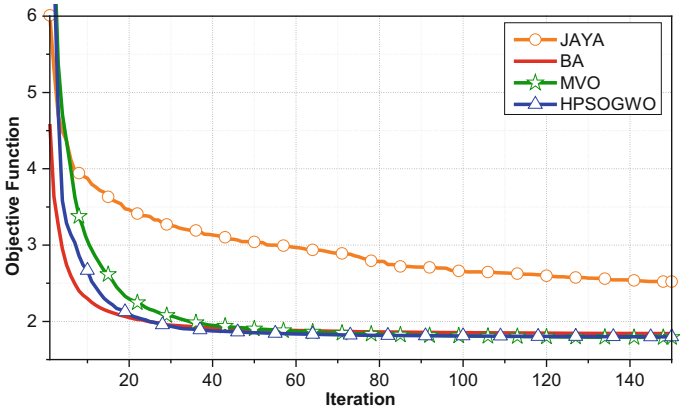

Fig. 9. Objective function of interferences suppression solutions with different algorithms

B. *Ability to eliminate single-interferences*

In Scenario 3, the radiation pattern is optimized with a single null. This null can be placed at any angle, and in this case, it is chosen at the peak of the second sidelobe (14°). The individuals were initialized as Chebyshev array weights with an SLL of −30dB.

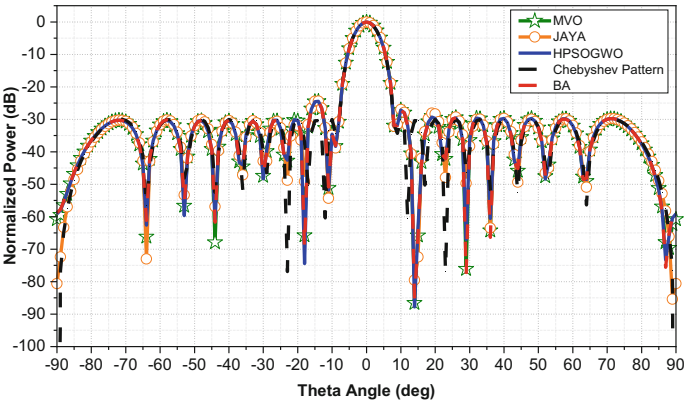

Fig. 10. Optimized patterns with a single null at 14°

In [11], Haupt made a significant discovery that the phase has a more substantial impact on the main beam compared to the amplitude, and introducing slight phase perturbations during nulling will not significantly degrade the main beam. Additionally, a smaller phase weighting range leads to a faster convergence rate. Hence, during the simulation process for all radiation pattern adjustment scenarios, the phase weight variations were confined to the range from −0.1 to 0.1 radians. Figure 10 displays the optimized radiation patterns with a single null obtained using the BA, HPSOGWO, MVO, and Jaya algorithms. These algorithms successfully retain almost all the characteristics of the original Chebyshev pattern, such as the half-power beamwidth *(HPBW = 7.64°)* and *Sidelobe Level (SLL)* of −30 dB, except for a few sidelobes exhibiting an approximate maximum SLL of −20 dB. Notably, the depth of the null point (NDL) at 14° is −87.8 dB, −87.8 dB, −85 dB, and −79.5 dB, respectively, for HPSOGWO, MVO, BA, and Jaya algorithms. These results clearly demonstrate the high effectiveness of interference suppression achieved by accurately placing null points at interference directions using metaheuristic algorithms.

C. *Ability to eliminate Multiple-interferences*

In Scenario 4, the radiation pattern is optimized with multiple individual nulls located at angles −48°, 20°, and 40°, corresponding to the peaks of the next three sidelobes after the main beam in the Chebyshev array radiation pattern. Figure 11 displays the optimized radiation patterns with multiple nulls obtained using the BA, HPSOGWO, MVO, and Jaya algorithms. These algorithms effectively preserve almost all the characteristics of the original Chebyshev pattern, including the half-power beamwidth (HPBW = 7.64°) and Sidelobe Level (SLL) of −30 dB, with only a few sidelobes exhibiting an approximate maximum SLL of −20 dB. The NDL at −48°, 20°, and 40° is presented in Table 1, demonstrating that all NDL values are deeper than −73 dB and all SLL values are lower than −20 dB, while the HPBW remains close to the Chebyshev pattern. These results further illustrate the interference suppression and cancellation capabilities of metaheuristic algorithms in this scenario.

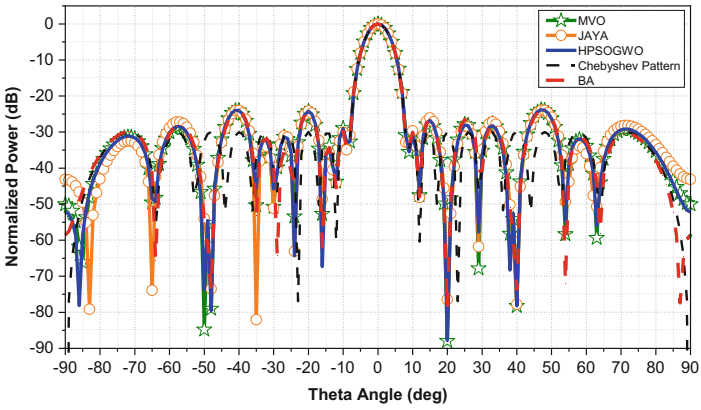

Fig. 11. Optimized patterns with three nulls at −48°, 20°, and 40°

Table 1. Null Depth Level in Fig. 11

Parameters	BA (dB)	HPSOGWO (dB)	MVO (dB)	Jaya (dB)
NDL at:-48^o	−74.2	−79.5	−79.5	−74.2
NDL at: 20^o	−79.5	−87.8	−88	−79.5
NDL at: 40^o	−73.6	−78.2	−77.8	−77.7

D. *Ability to eliminate Broad-interferences*

In interference suppression applications, a broad null becomes essential when the Directions of Arrival (DOA) of interferences slightly vary with time, are not precisely known, or when continuous null steering is required to achieve an appropriate signal-to-noise ratio. To showcase the capability of broad interference suppression, in Scenario 4, a pattern has been generated with an imposed broad null covering the target sector of [30°, 40°]. This pattern is depicted in Fig. 12.

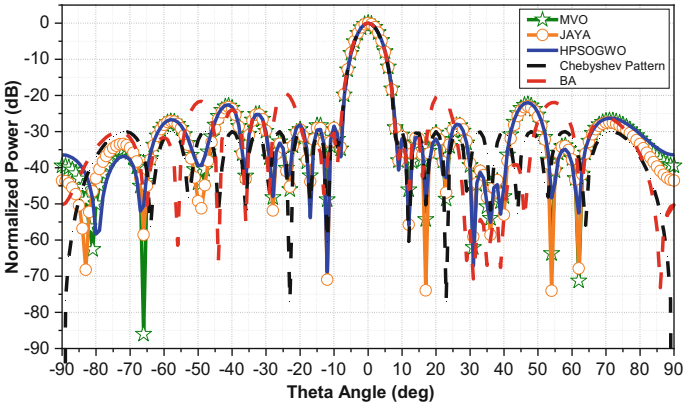

Fig. 12. The optimized patterns exhibit a broad null spanning from 30° to 40°

The main beamwidth remains nearly unchanged, and the maximum Sidelobe Level (SLL) is approximately –20 dB. The results demonstrate that the BA pattern outperforms HPSOGWO, MVO, and Jaya in terms of *NDL,* with wide null and NDL values reaching a minimum of < -53.9 dB, -41.3 dB, 40.9 dB, and 40.9 dB, respectively, for the BA, HPSOGWO, MVO, and Jaya patterns.

E. *Patterns with Mutual Coupling*

Scenario 6 is used to explore the impact of mutual coupling on the radiation pattern optimized by MVO.

To achieve this, the influence of mutual coupling is computed using the mutual impedance matrix presented in Sect. 2, and Fig. 13 illustrates the simulation results for the case of placing multiple nulls simultaneously, with results summarized in Table 2.

The results have indicated that the nulls have been successfully placed at the desired positions, but with a shallower NDL and more challenging control of the sidelobes at around −30 dB, although the main lobe is still maintained.

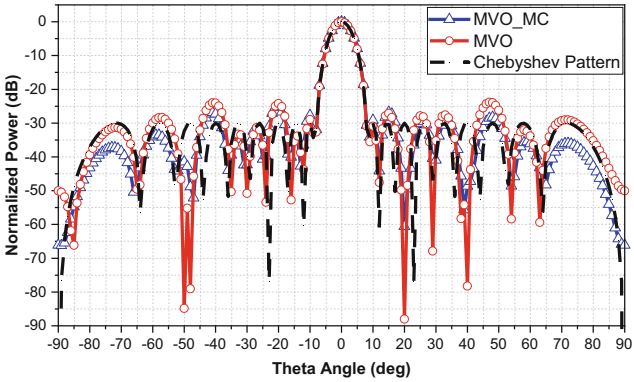

Fig. 13. The optimized pattern (with nulls at angles −48°, 20°, and 40°) accounting for mutual coupling effects

Table 2. Null Depth Level in the Fig. 13

Parameters	Null at: −48°		Null at: 20°		Null at: 40°	
Algorithm	MVO	MVO-MC	MVO	MVO-MC	MVO	MVO-MC
NDL (dB)	−79	−48.8	−88	−60.6	−78.3	−48.6

F. *The radiation pattern when steering the main beam*

The beamformer can also steer the main beam in any direction in space. To achieve this, before proceeding with the search for optimal weights, the Chebyshev radiation pattern in the objective function needs to be steered in the desired direction. In this scenario, the main beam is steered towards $\theta^0 = 10^0$ while setting various types of nulls, as illustrated in Fig. 14.

The results indicate that interference suppression solutions based on metaheuristic algorithms can still perform well, as presented in the cases above. Specifically, the main beam is preserved almost similarly to the main beam of the Chebyshev radiation pattern, and the majority of the SLL is controlled at around −30 dB, except for some sidelobes at approximately −20 dB due to the odd-symmetry nature of the phase-only control technique.

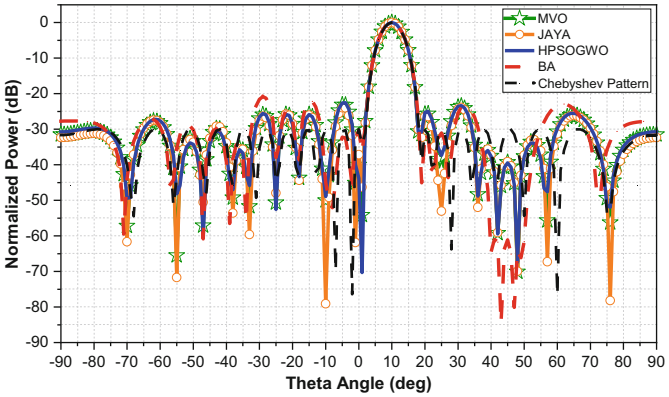

Fig. 14. The optimized radiation patterns when steering the main beam.

G. *Change the number of antenna elements in the antenna array to evaluate the solution*

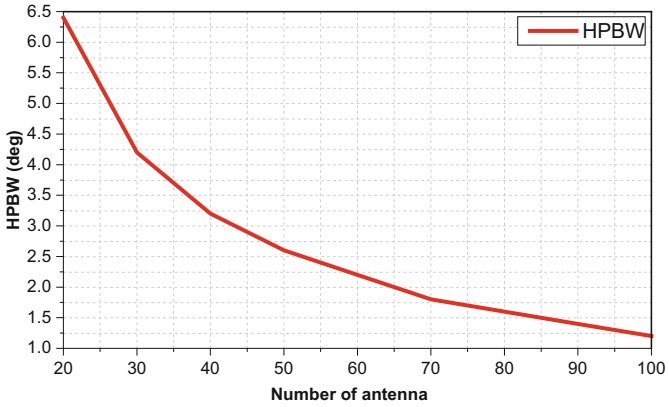

Fig. 15. HPBW versus the number of array antenna elements

Scenario 8 is designed to comprehensively evaluate the impact of varying the number of antenna elements in the array on essential performance parameters, namely HPBW, FNBW, NDL, and MaxSLL. The results of this scenario are displayed in four graphs that unravel the dynamic relationship between key performance metrics (HPBW, FNBW, NDL, and MaxSLL) and antenna element counts, providing an in-depth analysis. About the multifaceted interaction between antenna array size and BF performance. We investigate the relationship between each parameter and the number of antenna elements, which varies from 20 to 100 elements with penalty parameters is 10000 and based on the MVO algorithm.

Figure 15 and 16, which depict the relationship between antenna elements and HPBW and FNBW, respectively, contribute significantly to our comprehension. Within these

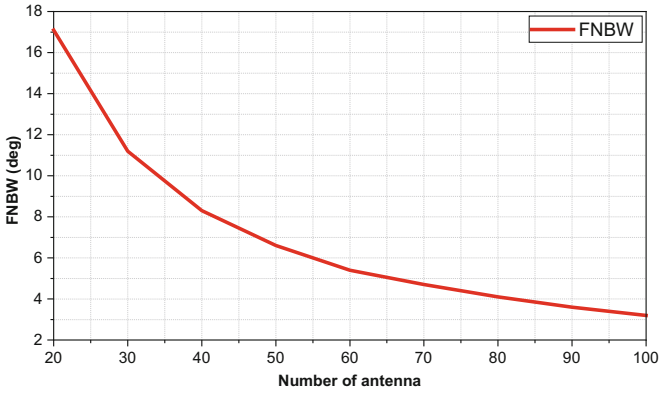

Fig. 16. FNBW versus the number of array antenna elements

visuals, an intriguing pattern comes to the fore: both HPBW and FNBW exhibit a tendency to narrow, signalling the enhanced capabilities of larger arrays in terms of more precise main lobe concentration and improved angular precision.

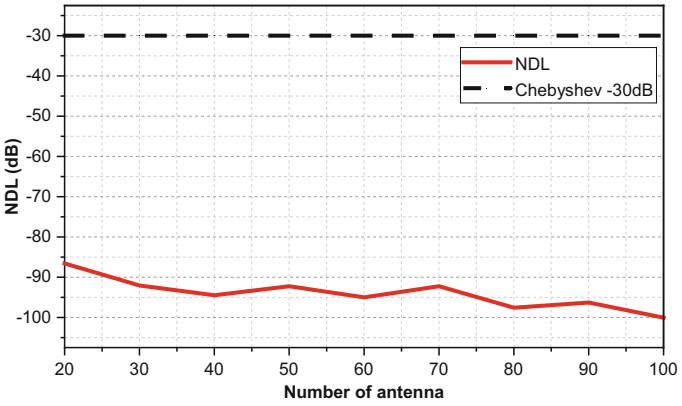

Fig. 17. NDL versus the number of array antenna elements

Observing the graph in Fig. 17, we discern a noteworthy trend: as the number of antenna elements increases, the null point depth experiences a consistent improvement. This trend underscores the pivotal role of spatial diversity in array configurations, where a larger number of elements empowers BF algorithms to more precisely nullify interference and noise from specific angles. The upward trajectory of null point depth with growing array size holds immense promise for enhancing signal clarity, target localization, and noise suppression in a wide array of applications.

In Fig. 18, as the number of antenna elements increases, the graph shows a marked decrease at the maximum side-beam level. This phenomenon highlights the benefit of a larger antenna array in reducing signal leakage and unwanted radiation away from the main lobe.

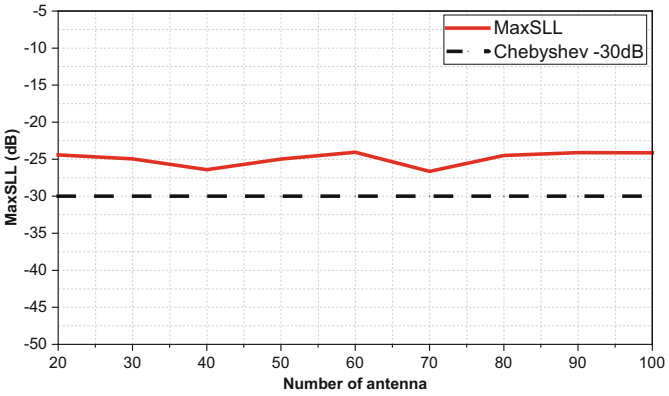

Fig. 18. MaxSLL versus the number of array antenna elements

While a larger antenna array delivers improvements in null point depth, sidelobe reduction, and angular precision, there is a point of diminishing returns. Beyond a certain array size, the benefits may become marginal, and concerns such as hardware complexity, cost, and signal processing burden come to the fore. Industries such as telecommunications, aerospace, and defense have distinct metrics based on their unique requirements. Therefore, the pursuit of an optimal array size necessitates a holistic approach, balancing technical advancements, practical constraints, and specific needs. In conclusion, four graphs provide a panoramic view of the intricate synergy between performance metrics and the number of antenna elements in BF. As researchers and practitioners look for better BF solutions, this relationship acts as a guide, showing them how to find array configurations that make the most of null point depth, sidelobe suppression, angular accuracy, and null beamwidth. This will shape the future of signal enhancement and noise suppression.

4 Conclusion

In this study, we looked at how to get rid of interference using metaheuristic algorithms and controlling the excitation signal's phase only for each antenna element in the array. The interference suppression capability was demonstrated through eight scenarios, including convergence rate, placing single null, multiple nulls, and broad nulls on the radiation pattern in an ideal case, the impact of interference, steering the main beam, and increasing the number of antenna elements. The results demonstrate that the solution can precisely apply the aforementioned nulls to any arbitrary interference direction while maintaining low sidelobe levels and the main lobe in both circumstances of mutual coupling. Moreover, solutions based on BA, HPSOGWO, and MVO demonstrate superior efficiency compared to Jaya-based ones in terms of computation time, pattern nulling, and sidelobe suppression during antenna array radiation pattern synthesis. In this paper, we examine this solution within the context of 5G. However, the outcomes also highlight its potential applicability and suitability for future 6G technology. In the

future, solutions for unknown interference directions based on different optimization techniques, such as convex optimization or deep learning, will be further explored.

References

1. Wang, D., Chen, D., Song, B., Guizani, N., Yu, X., Du, X.: From IoT to 5G I-IoT: the next generation IoT-based intelligent algorithms and 5G technologies. IEEE Commun. Mag. **56**(10), 114–120 (2018). https://doi.org/10.1109/MCOM.2018.1701310
2. Quy, V.K., Hau, N.V., Anh, D.V., Ngoc, L.A.: Smart healthcare IoT applications based on fog computing: architecture, applications and challenges. Complex Intell. Syst. **8**(5), 3805–3815 (2022). https://doi.org/10.1007/s40747-021-00582-9
3. Khanh, Q.V., Hoai, N.V., Manh, L.D., Le, A.N., Jeon, G.: Wireless communication technologies for IoT in 5G: vision, applications, and challenges. Wirel. Commun. Mob. Comput. **2022**, 1–12 (2022). https://doi.org/10.1155/2022/3229294
4. Chettri, L., Bera, R.: A comprehensive survey on internet of things (IoT) toward 5G wireless systems. IEEE Internet Things J. **7**(1), 16–32 (2020). https://doi.org/10.1109/JIOT.2019.2948888
5. Kha, H.M., Luyen, T.V., Cuong, N.V.: An efficient beamformer for interference suppression using rectangular antenna arrays. J. Commun. **18**(2), 116–122 (2023)
6. Siddiqui, M.U.A., Qamar, F., Ahmed, F., Nguyen, Q.N., Hassan, R.: Interference management in 5G and beyond network: requirements, challenges and future directions. IEEE Access **9**, 68932–68965 (2021). https://doi.org/10.1109/ACCESS.2021.3073543
7. Shafique, K., Khawaja, B.A., Sabir, F., Qazi, S., Mustaqim, M.: Internet of things (IoT) for next-generation smart systems: a review of current challenges, future trends and prospects for emerging 5G-IoT scenarios. IEEE Access **8**, 23022–23040 (2020). https://doi.org/10.1109/ACCESS.2020.2970118
8. Luyen,T.V., Cuong, N.V., Giang, T.V.B.: Convex optimization-based sidelobe control for planar arrays. In: 2023 IEEE Statistical Signal Processing Workshop (SSP), Hanoi, Vietnam, pp. 304–308 (2023)
9. Zhu, X., Qi, F., Feng, Y.: Deep-learning-based multiple beamforming for 5G UAV IoT networks. IEEE Netw. **34**(5), 32–38 (2020). https://doi.org/10.1109/MNET.011.2000035
10. Trees, H.L.V.: Optimum Array Processing: Part IV of Detection, Estimation, and Modulation Theory. Wiley, New York (2002)
11. Haupt, R.L.: Antenna Arrays: A Computational Approach. John Wiley & Sons, Hoboken (2010)
12. Kha,H.M., Luyen, T.V., Cuong, N.V.: A null synthesis technique-based beamformer for uniform rectangular arrays. In: 2022 International Conference on Advanced Technologies for Communications (ATC), pp. 13–17 (2022)
13. Luyen,T.V., et al.: An efficient ULA pattern nulling approach in the presence of unknown interference. J. Electromagn. Waves Appl., 1–18 (2021)
14. Agrawal, P., Abutarboush, H.F., Ganesh, T., Mohamed, A.W.: Metaheuristic algorithms on feature selection: a survey of one decade of research (2009–2019). IEEE Access **9**, 26766–26791 (2021). https://doi.org/10.1109/ACCESS.2021.3056407
15. Yang, X.-S.: Nature-Inspired Optimization Algorithms, pp. 141–154. Elsevier, Oxford (2014)
16. Thuc, K.X., Kha, H.M., Cuong, N.V., Luyen, T.V.: A Metaheuristic-based hyperparameter optimization approach to beamforming design. IEEE Access **11**, 52250–52259 (2023). https://doi.org/10.1109/ACCESS.2023.3277625
17. Singh, N., Singh, S.B.: Hybrid algorithm of particle swarm optimization and grey wolf optimizer for improving convergence performance. J. Appl. Math. **2017**, 2030489 (2017). https://doi.org/10.1155/2017/2030489

18. Mirjalili, S., Mirjalili, S.M., Hatamlou, A.: Multi-Verse optimizer: a nature-inspired algorithm for global optimization. Neural Comput. Appl. **27**(2), 495–513 (2016). https://doi.org/10.1007/s00521-015-1870-7
19. Rao,R.V.: Jaya: a simple and new optimization algorithm for solving constrained and unconstrained optimization problems. Int. J. Ind. Eng. Comput. (2016). https://www.scilit.net/article/c9341fa01676ca42c8b2157ec8847c37
20. Balanis, C.A.: Antena Theory: Analysis and Design. Wiley, Hoboken (2016)
21. Orfanidis,S.J.: Electromagnetic waves and antennas (2016)
22. Shore, R.: A proof of the odd-symmetry of the phases for minimum weight perturbation phase-only null synthesis. IEEE Trans. Antennas Propag. **32**(5), 528–530 (1984). https://doi.org/10.1109/TAP.1984.1143351
23. Luyen,T.V., et al.: An approach of utilizing binary bat algorithm for pattern nulling. In: Solanki, V., Hoang, M., Lu, Z., Pattnaik, P. (eds.) Intelligent Computing in Engineering. Advances in Intelligent Systems and Computing, vol. 1125. Springer, Singapore (2020). https://doi.org/10.1007/978-981-15-2780-7_101
24. Yeniay, Ö.: Penalty function methods for constrained optimization with genetic algorithms. Math. Comput. Appl. **10**, 45–56 (2005). https://doi.org/10.3390/mca10010045
25. Tong, L., Nguyen, C., Le, D.: An effective beamformer for interference mitigation. In: Anh, N.L., Koh, S.J., Nguyen, T.D.L., Lloret, J., Nguyen, T.T. (eds.) Intelligent Systems and Networks. Lecture Notes in Networks and Systems, vol. 471, pp. 630–639. Springer, Singapore (2022). https://doi.org/10.1007/978-981-19-3394-3_73
26. Dolph, C.L.: A current distribution for broadside arrays which optimizes the relationship between beam width and side-lobe level. Proc. IRE **34**(6), 335–348 (1946). https://doi.org/10.1109/JRPROC.1946.225956